

2015

Energy harvesting in a diver's rebreather system

Ely, J.

Ely, J. (2015) 'Energy harvesting in a diver's rebreather system', The Plymouth Student Scientist, 8(2), p. 85-114.

<http://hdl.handle.net/10026.1/14098>

The Plymouth Student Scientist
University of Plymouth

All content in PEARL is protected by copyright law. Author manuscripts are made available in accordance with publisher policies. Please cite only the published version using the details provided on the item record or document. In the absence of an open licence (e.g. Creative Commons), permissions for further reuse of content should be sought from the publisher or author.

Energy harvesting in a diver's rebreather system

Joseph Ely

Project Advisor: Dan Hatton, School of Marine Science and Engineering, Plymouth University, Drake Circus, Plymouth, PL4 8AA

Abstract

This report investigates the feasibility of energy harvesting using thermoelectric generators in a diver's rebreather system. The report details research into documented experiments and theory, design and manufacture of an energy harvesting prototype and testing of the prototype to determine its feasibility. The prototype produced a maximum power of 2.5 (mW) which is more than the minimum 50 microwatts of power specified by Avon. It was therefore concluded that energy harvesting within a divers rebreather system is feasibility.

1 Acknowledgements

I would like to thank Frazer Ely for his guidance and mentoring throughout the project; Nick Bushel at Avon underwater systems for his teaching, support and enthusiasm. I would like to thank Dr Dan Hatton for his helpful and positive contributions throughout the project and aid in getting through the red tape; Stuart MacVeigh for his expertise and practical ability aiding in the electronics of the project; Dr Richard Cullen for his expertise and aid in adhesives and sealants; and Bob Williams for his expertise and aid in 3D printing.

2 Contents

1	Acknowledgements.....	86
3	List of figures.....	87
4	List of tables.....	88
5	Introduction.....	89
5.1	Aims.....	89
5.2	Objectives.....	89
5.3	Changes in Aims and Objectives.....	89
5.3.1	Thermodynamic model.....	89
5.3.2	Requirements of the client.....	90
6	Project timescale.....	90
7	Energy harvesting methods summary and Evaluation.....	92
7.1.1	Electrostatic droplet jumping.....	92
7.1.2	Kinetic.....	92
7.1.3	Thermoelectric.....	92
7.2	Evaluation.....	92
7.2.1	Calculations.....	92
8	Thermoelectric Energy Harvesting Background.....	93
8.1	General Thermoelectric theory.....	93
8.2	How a thermoelectric generator work.....	93
8.3	Design and materials.....	93
9	Mathematical Models.....	94
9.1	Thermal Resistance network diagrams and components.....	94
9.2	Thermal resistance network efficiency and graphing.....	95
9.3	Mathematical model.....	96
10	Design and manufacture.....	99
10.1	Introduction.....	99
10.2	The Prototype.....	99

10.2.1	Brief Design Specification	99
10.3	The design	100
10.3.1	Details	100
10.4	Materials and manufacture	100
10.5	Manufacturing Limitations.....	101
10.6	Design Drawings.....	102
10.7	Design Future recommendations	103
11	Experiment.....	103
11.1	Introduction	103
11.2	Aims.....	103
11.3	Methodology.....	103
11.3.1	Apparatus.....	103
11.3.2	Set up	104
11.3.3	Execution.....	105
11.3.4	Safety	105
11.4	Variables.....	105
11.5	Prediction	106
11.6	Results.....	106
11.7	Graphs.....	106
11.8	Conclusion.....	108
11.8.1	Description of the results.....	108
11.8.2	Scientific explanation for the results	109
11.8.3	Conclusion from results	110
11.8.4	Do results agree with the prediction?	110
	Evaluation	110
11.8.5	Validity	110
11.8.6	Accuracy and precision	111
11.8.7	Future recommendations	111
12	Project conclusion.....	111
13	References	112

3 List of figures

Figure 1	Gantt Chart	91
Figure 2	Diagram of thermal resistance network	94
Figure 3	thermal resistance network and reffrence diagram	94
Figure 4	Thermal resistance network	95

Figure 5 power output from mathematical model.....	98
Figure 6 Efficiency of TEG from mathematical model.....	98
Figure 7 power outputs for reliability comparison	99
Figure 8 teg selectiong graph.....	100
Figure 9 defective part	101
Figure 10 exploded view of prototype.....	102
Figure 11 top view of prototype	102
Figure 12 underside of prototype	102
Figure 13 clamp bars	102
Figure 14 scale of prototype.....	102
Figure 15 Experimental set up	104
Figure 16 Experimental prototype	104
Figure 17 experimental rebreather	105
Figure 18 experiment voltage graph.....	107
Figure 19 experiment amplitude graph.....	107
Figure 20 experiment power graph.....	108
Figure 21 experiment thermocouple graph.....	108

4 List of tables

Table 1 Feasibility calculation values	93
Table 2 Thermal resistance references	95
Table 3 Coefficients	97

5 Introduction

A rebreather is a self-contained life support system that provides breathable air for a diver. It is a closed loop system that recirculates and controls the divers breathing gas, adding oxygen and removing CO₂ (Sentinel rebreather Manual, n.d.) (Wikipedia, 2015). The CO₂ is removed by Soda Lime or Ca(OH)₂ (Wikipedia, 2015) (Chemical Book, 2010). The soda lime is held in a canister called the “scrubber” (Sentinel rebreather Manual, n.d.) (Wikipedia, 2015).

The rebreather requires batteries to power electrical systems for gas sensors and controls (Sentinel rebreather Manual, n.d.) (U. S. Department of the Navy, Naval Sea Systems Command, 2008). Talks with Avon Representatives revealed that this possesses an inherent problem as these batteries are required to be replaceable and cause weak spots in the diving design, often requiring cabling and connectors to remote sensors. These weak spots can result in leaks due to the high pressures experienced at depth. By removing the need for these batteries and providing an energy harvesting alternative one could improve the reliability and ease of use of the rebreather. A potential energy source is the thermal energy in the diver’s breath, which is recirculated around the breathing loop in a rebreather.

This project is run with the support of Avon Underwater Systems, who design and supply subsea equipment and specialise in rebreathers.

5.1 Aims

- Determine the feasibility of energy harvesting applications within a diver’s life support system to power sensors or controls.

5.2 Objectives

- Identify the energy harvesting method that has the highest energy production potential through feasibility calculations.
- Produce a mathematical model to predict the power output of the energy harvesting method.
- Produce a prototype/experimental test piece and determine its power output through experiment.
- Determine if the energy harvesting application is a feasibility by showing the prototype can generate a minimum of 50 micro watts.

5.3 Changes in Aims and Objectives

5.3.1 Thermodynamic model

The first major shift in the project aims and objectives was before the project proposal phase. Initially a thermodynamic model of the rebreather was planned so that an optimum positioning of the thermoelectric plates could be decided on. A thermodynamic model would have been too time consuming to incorporate within a single project alongside the determination of the feasibility of energy harvesting therefore Avon background knowledge, research and calculations should be sufficient to replace this method. A fellow student is undertaking the thermodynamic modelling side of the project so that the model will be able to be used by Avon for future improvements.

5.3.2 Requirements of the client

Since the start of the project the focus of the project has moved from creating a fully developed prototype to producing the required data in order to implement a thermoelectric system. This is due to discussions with representatives of Avon Resulting in the idea that the data would be more useful to them rather than a specific prototype which only fits a certain model of rebreather.

From Background Research into commercially available thermoelectric generators it has become clear that specific shaping of thermoelectric generators is difficult due to the complex nature of the generator itself therefore generating specific dimensions may be out of the scope of this project. The objective of “generating a prototype of the energy harvesting device” will be changed to “Generating a prototype/experimental device to generate relevant data”. Testing a prototype has been changed to testing prototype/experimental device.

6 Project timescale

Time spent on the project was placed in 3 main areas firstly research then design and manufacture of prototype and then experiment testing. The manufacture and design stage took significantly longer than originally expected this was due to limitations in the methodology such as; a large number of iterations on the design, budget issues with regards 3D printing and manufacturing defects from the printer itself. The experimental testing stage also took longer than anticipated this was due to data logging for the voltage readings not being readily available and hence a more complex system had to be programed into a myDAQ computer. These extensions can be seen in figure 1 along with the overall project timescale.

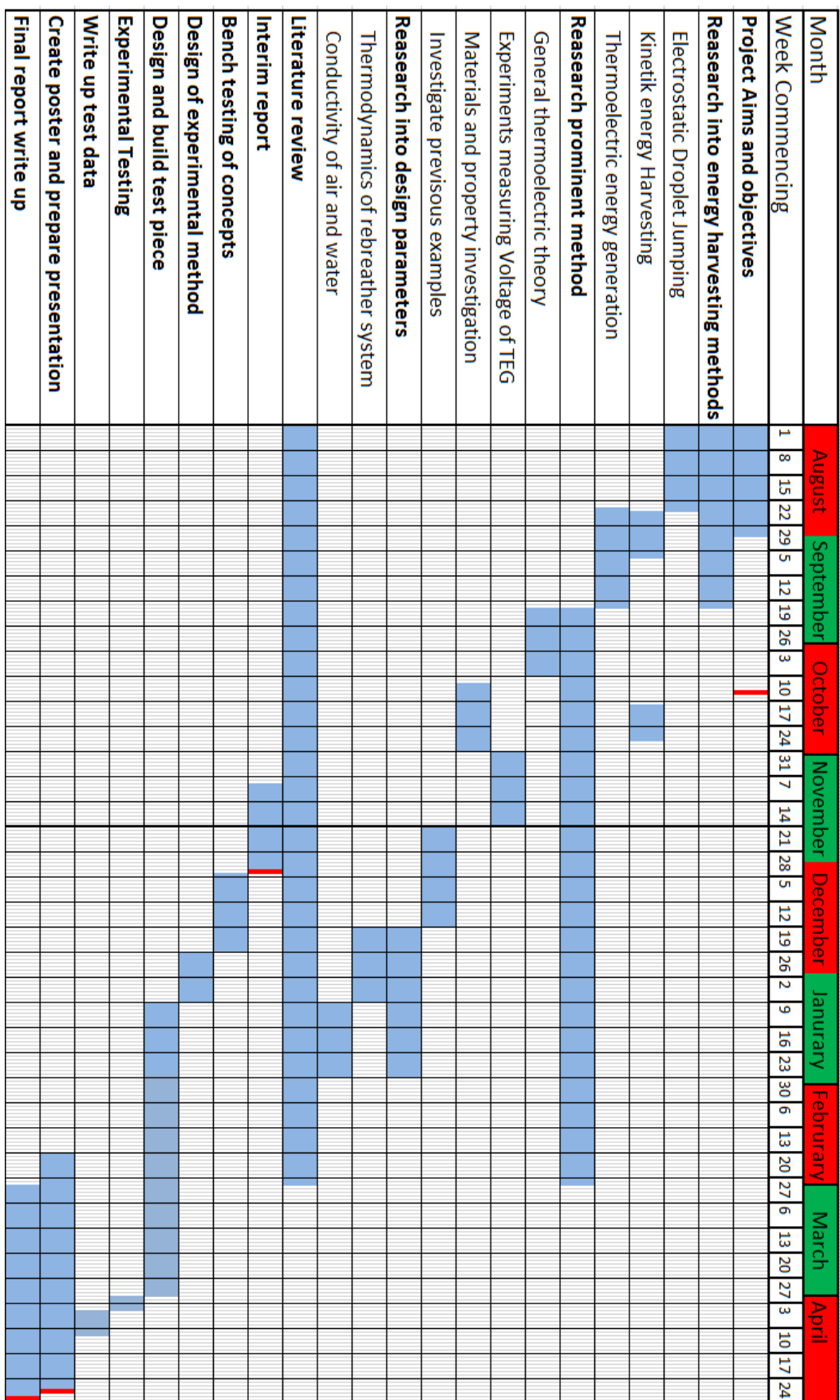


FIGURE 1 GANTT CHART

7 Energy harvesting methods summary and Evaluation

A range of energy harvesting methods were researched from (Dewan, et al., 2014) and (Paradiso & Starner, 2005) such as the ones below and additional methods that did not reach the shortlisting stage after qualitative assessment (see appendix A. Feasibility Calculations were then carried out on potential methods to determine the most effective method to move forwards with. The calculations can be seen in appendices.

7.1.1 Electrostatic droplet jumping

This technology harvests the latent heat of evaporation to create electrical charge in droplets which jump from a super hydrophobic plate to a super hydrophilic plate “due to the release of excess surface energy” (Miljkovic, et al., 2013) to create a circuit.

7.1.2 Kinetic

Research into Kinetic energy harvesting revealed Delvanez’ (2012) paper on “electromagnetic micro power generator for energy harvesting from breathing” which highlighted the use of a mask device which the user would breathe into and the kinetic energy in the breath would be harvested. The paper stated that breath pressure was “2% higher than ambient” which corresponds to “1W of power”.

7.1.3 Thermoelectric

This technology harvests the thermal energy in air via thermo-electrical materials applied to a temperature difference which causes a flow of electrons “through the Seebeck effect” (Cengel & Boles, 1998).

7.2 Evaluation

Requirements	
<ul style="list-style-type: none"> Produce maximum amount of power Can operate under water and under pressure Will consistently produce the power 	<ul style="list-style-type: none"> is not overly large e.g. 1m³ does not provide discomfort to the diver (breathing difficulty)

7.2.1 Calculations

The feasibility calculations predict how much available energy there is to harvest using each harvesting method. One thing to note is that the feasibility studies do use large approximations for example assuming there are 2 litres of air in each breath and that the conditions are standard sea level conditions whereas the diver would actually be under water. The calculations are therefore ballpark or order of magnitude calculations for further details see appendix B.

TABLE 1 FEASIBILITY CALCULATION VALUES

Method	Electrostatic droplet Jumping	Thermoelectric	Kinetic pressure	Kinetic breathing force
Power available (W)	35	43	1	4.12×10^{-3}

As can be seen from Table 1 thermoelectric energy generation generates the most power at 43 watts further after a process of reduction was placed on matching the requirements to the technology (see appendix C) showing that thermoelectric energy harvesting provides the best solution.

8 Thermoelectric Energy Harvesting Background

8.1 General Thermoelectric theory

Summarising Cengel & Boles' (1998) section on thermoelectric principle: The generator operates under the phenomena called the Seebeck effect discovered by Thomas Seebeck in 1821. This is where a current is produced as a result of a temperature difference. The major drawback in thermoelectric devices in their current state is their low efficiency as can be seen in the equations below and also (Cengel & Boles, 1998). However they can and have still produced useful power as seen in there "use on the voyager spacecraft in 1980" (Cengel & Boles, 1998). Further the marginal cost of the energy input is 0 as the energy comes from a diver's breathing therefore financially they are highly efficient as their cost is only implementation and maintenance. Thermoelectric devices have very high reliability (Cengel & Boles, 1998) so maintenance would likely be a small cost.

8.2 How a thermoelectric generator work

Thermoelectric harvesters utilise 2 dissimilar semiconductors Labelled N and P conductors these conductors are doped so that one has 1 extra valance electron per dopant atom and one has one fewer. The extra or missing valance electrons cause the semiconductor to become conductive through negative and positive charge carriers (Tellurex, 2010).

When there is a flow of heat over the semiconductors the charge carrier is set into motion in the same direction as the heat through the Seebeck effect. This can be designed into an electrical circuit through the use of the positively and negatively doped semiconductors. Therefore semiconductors are connected thermally in parallel but electrically in series (Rowe, 1994).

8.3 Design and materials

Rowe (1994) states that the power output from a thermoelectric couple is approximately proportional to its area and inversely proportional to its length therefore modules need a large amount of thermocouples with very small widths.

There is a wide variety of thermoelectric materials available but at the most there are 3 that are commonly used and are available commercially. These are "Lead Telluride

(PbTe), Silicon Germanium (SiGe), and Bismuth-Antimony (Bi-Sb) alloys” (Ferrotec, n.d.).

Bismuth has the highest figure of merit (as described in the section above, and in the temperature range that will be experienced whilst diving 0 – 30°C) out of all the common thermoelectric materials. Using Bismuth as a thermoelectric generator also seems to be the material of choice backed by Goldsmid (2014) who stated “it is the best material for use at room temperature, and Chung et al. (n.d.) who stated that it has a dimensionless figure of merit between 0.8 and 1 at room temperature. Therefore the experimental test piece will utilise a bismuth telluride module.

9 Mathematical Models

9.1 Thermal Resistance network diagrams and components

A thermal resistance network was set up to predict the thermal energy transfer over the thermal network shown in figure 3. The components of the Prototype are connected thermally in parallel this can be seen in figure 2.

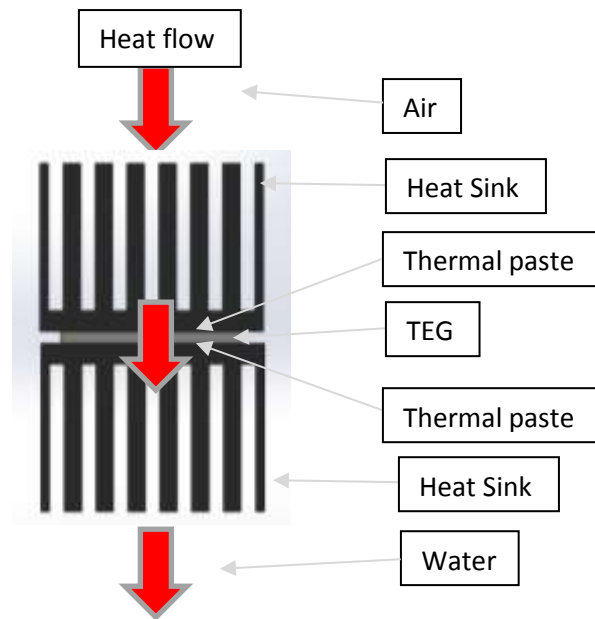


FIGURE 2 DIAGRAM OF THERMAL RESISTANCE NETWORK

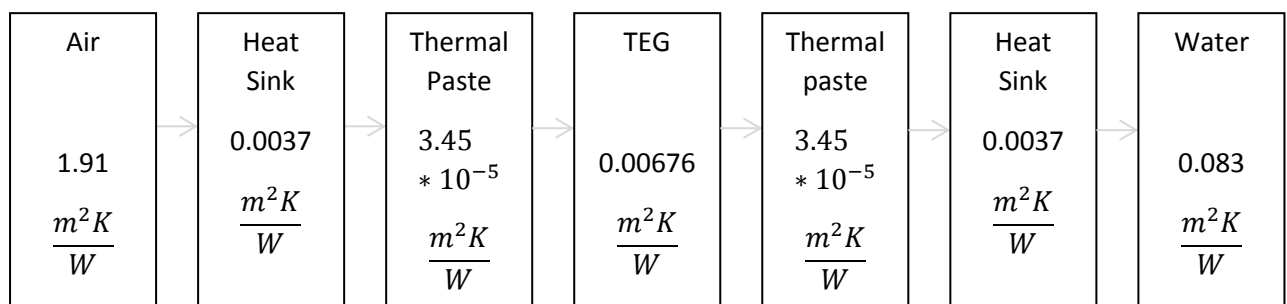


FIGURE 3 THERMAL RESISTANCE NETWORK AND REFERENCE DIAGRAM

TABLE 2 THERMAL RESISTANCE REFERENCES

Component	Reference
Air	(Haywood, 2005)
Heat sink	(AAVID THERMALLOY, n.d.)
Thermal paste	(Radio Spares, 2013)
Thermoelectric generator	(European Thermodynamics Limited , n.d.)
Water	(Haywood, 2005)

9.2 Thermal resistance network efficiency and graphing

Thermoelectric generators have a documented maximum efficiency from 0.1-8%. The likely efficiency for this experiment is predicted by the mathematical model below to be 0.5% as the efficiency decreases at lower temperatures. (Dewan, et al., 2013)

There could be another thermal resistance component in parallel from heat sink to heat sink this is the thermal resistance of construction for example how efficiently the heat sinks are clamped to the TEG and heat losses to casing (Kryotherm, n.d.).

The theoretical results produced from this thermal resistance network are displayed graphically below in figure 4.

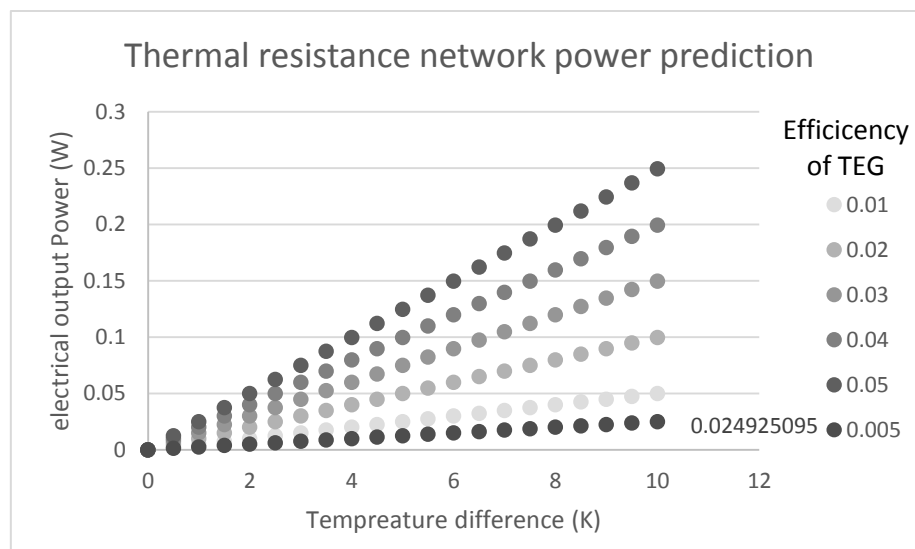


FIGURE 4 THERMAL RESISTANCE NETWORK

The graph in figure 8 suggests that over the predicted 10 degree temperature differential there should be 0.024925 Watts of power being generated at the efficiency predicted in figure 6 (0.5%).

9.3 Mathematical model

Nomenclature			
S	Seebeck coefficient	I	Is the maximum rated current for the particular TEG
DT	Temperature difference	N	Is the number of thermocouples
T	Temperature	K	Thermal conductance
R	Electrical resistance	P	Power
E	Efficiency		
Subscripts			
Th	Relates to the hot side of the module	1,2,3,4	Relates to the different coefficient from tests
Tc	Relates to the cold side of the module	New	Relates to the new value after converting to a different module
M	Means that this value relates to the module	O	Output
C	Refers to module	L	Refers to the Load

This model was created under the instruction from Ferrotec's documented technical advice section. The equations and data are reproduced from Ferrotec (2001). The model is based on test data collected by Ferrotec which is used to derive several "important coefficients" (such as the Seebeck coefficient the thermal conductance and the electrical resistance of the TEG). This test data was collected over a "comprehensive analysis of many thermoelectric cooling modules over a wide temperature range" (Ferrotec, 2001), therefore validating the coefficients. Note that Ferrotec used cooling modules for test data however these are exactly the same as power generating modules so this is not an issue.

Ferrotec did not release the data they recorded for use in creating the coefficients for polynomial interpolation as they were trying to produce a tool for mathematically modelling rather than a "highly detailed description of computer modelling techniques" (Ferrotec, 2001) meaning the validity of using the third order polynomials for interpolation is unclear.

Data is based on module operation in a normal air atmosphere with thermally conductive grease used at both hot and cold module interfaces. The data is valid over a range of -100°C to $+150^{\circ}\text{C}$.

Firstly the temperature dependent variables are determined from coefficients:

TABLE 3 COEFFICIENTS

Coefficients 71-cpl, 6-amp module					
Seebek		Thermal conductance		Electrical resistance	
1	1.33450×10^{-2}	1	4.76218×10^{-1}	1	2.08317
2	-5.37574×10^{-5}	2	-3.89821×10^{-6}	2	-1.98763×10^{-2}
3	7.42731×10^{-7}	3	-8.64864×10^{-6}	3	8.53832×10^{-5}
4	-1.27141×10^{-9}	4	2.20869×10^{-8}	4	-9.03143×10^{-8}

The coefficients are fed into the relevant third order polynomial equations below to produce the variables needed for performance analysis.

Seebek equation	Electrical resistivity equation	Thermal conductivity equation
$\frac{S_{MTh}}{S_{MTc}} = s_1T + \frac{s_2T^2}{2} + \frac{s_3T^3}{3} + \frac{s_4T^4}{4}$	$\frac{R_{MTh}}{R_{MTc}} = R_1T + \frac{R_2T^2}{2} + \frac{R_3T^3}{3} + \frac{R_4T^4}{4}$	$\frac{K_{MTh}}{K_{MTc}} = K_1T + \frac{K_2T^2}{2} + \frac{K_3T^3}{3} + \frac{K_4T^4}{4}$
Seebek over full module	Electrical resistance over full module	Thermal conductivity Over full module
$S_M = (S_{MTh} - S_{MTc}) / DT$	$R_M = (R_{MTh} - R_{MTc}) / DT$	$K_M = \frac{K_{MTh} - K_{MTc}}{DT}$
Correction Factors	Correction factors	Correction factors
$S_{new} = S_M * \frac{N_{new}}{71}$	$R_{new} = R_M * \frac{6}{I_{new}} * \frac{N_{new}}{71}$	$K_{new} = K_M * \frac{I_{new}}{6} * \frac{N_{new}}{71}$
Power output	Resistance of load	Current
$P_0 = \frac{(S_{new} * DT)^2}{4 * R_{new}}$	$R_L = 6 \text{ ohm}$	$I = \frac{S_{new} * DT}{R_{new} + R_L}$
Voltage	Heat input into the couple	Efficiency of module
$V = I * (R_{new} * R_c)$	$Q_h = (S_{new} * T_h * I) - (0.5 * I^2 * R_c) + (K_{new} * DT)$	$E = \frac{V * I}{Q_h}$

From this model the power output and module efficiency can be predicted over a range of temperature differences. The water temperature was kept at a constant 5°C and the hot air temperature was increased in 1 degree increments from this data graphs can be produced and used to predict performance.

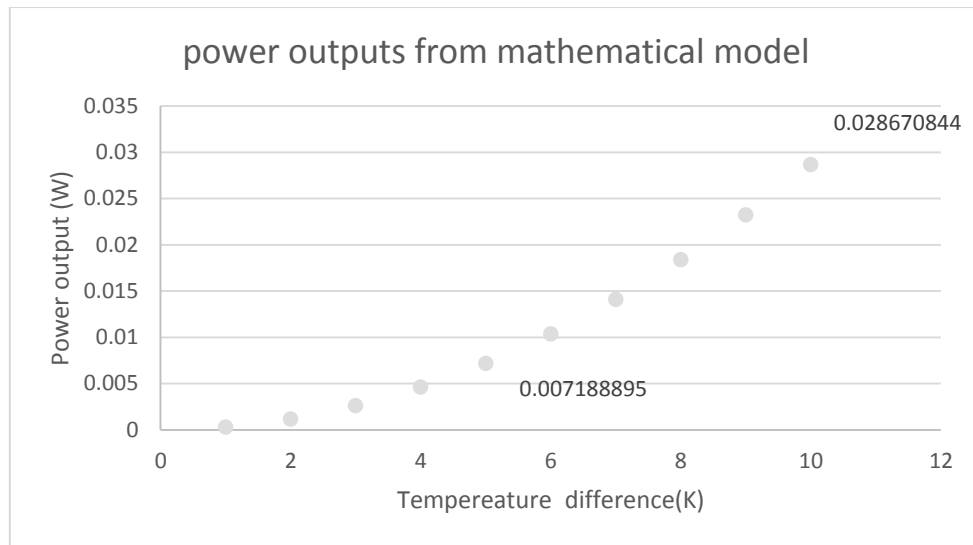


FIGURE 5 POWER OUTPUT FROM MATHEMATICAL MODEL

This mathematical model suggests that over a 10 degree temperature difference there will be 0.0287 W being generated (from figure 5) this is similar to 0.024925W predicted by the thermal resistance network approach.

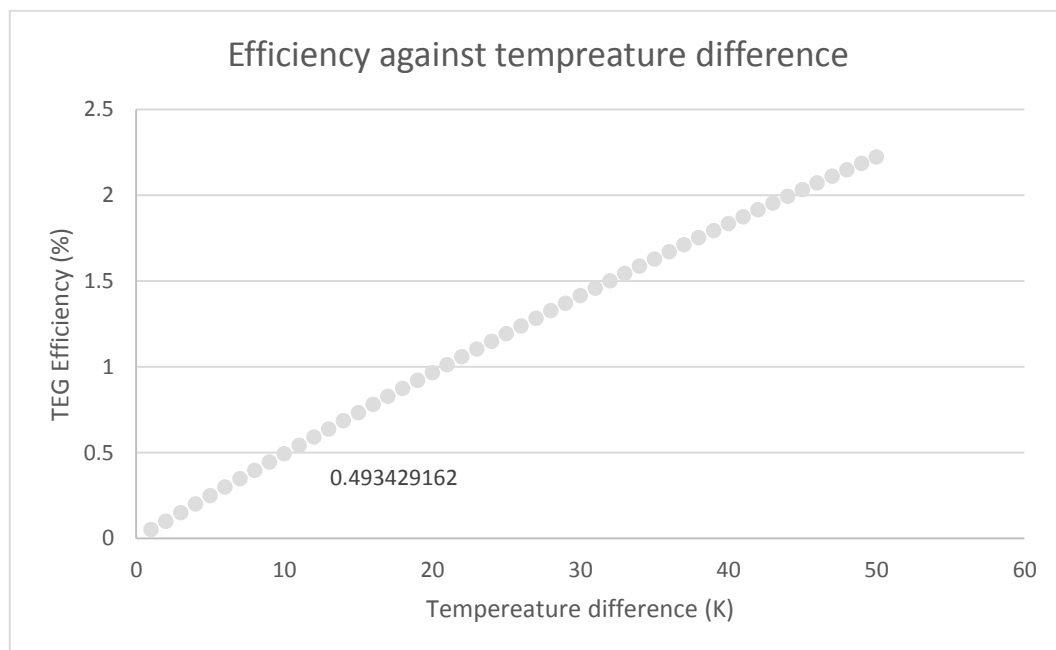


FIGURE 6 EFFICIENCY OF TEG FROM MATHEMATICAL MODEL

A published previous experiment showed power outputs of 0.11 watts at a 20° temperature difference compared to the O'Halloran (2014) paper. If the mathematical model is extended up to the same temperature differential at 20° then a power output of 0.114 watts can be seen, as shown in figure 7. The values from the experiment follow the trend of the Ferrotec model very closely validating the mathematical model.

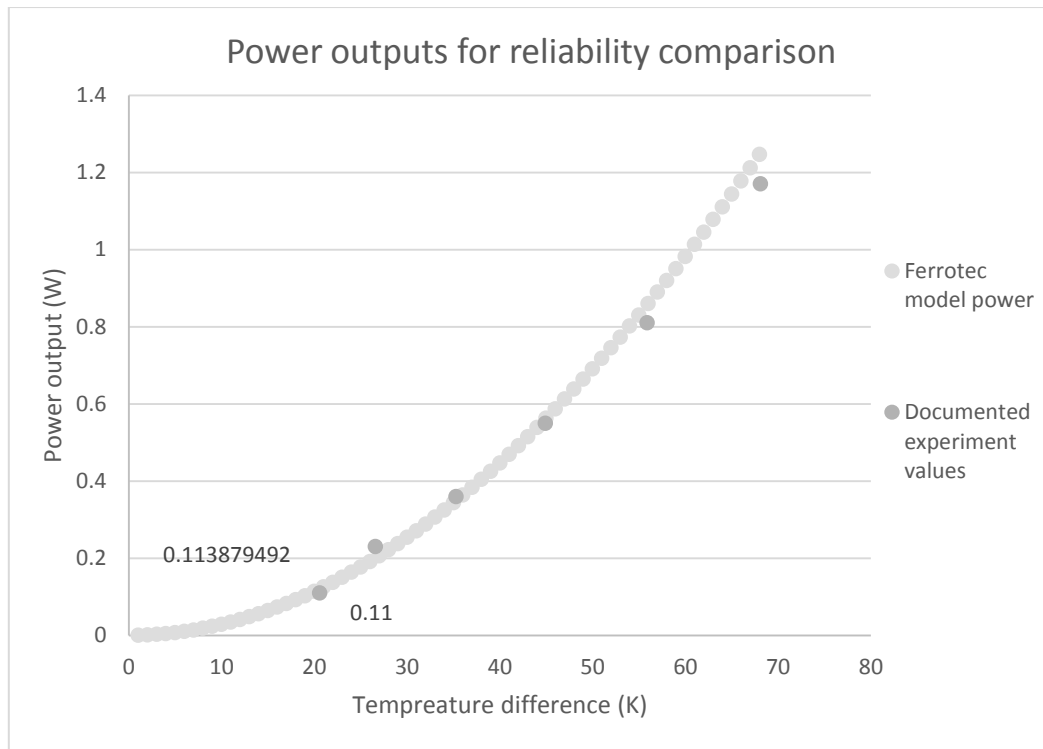


FIGURE 7 POWER OUTPUTS FOR RELIABILITY COMPARISON

10 Design and manufacture

10.1 Introduction

In order to assess the Feasibility of energy harvesting from a diver's breath an experiment was setup to measure the voltage produced over a load resistor by a prototype energy harvester. The temperature throughout the rebreather was also measured instantaneously for voltage temperature comparisons.

10.2 The Prototype

The prototype energy harvester was used as an experimental test piece to determine the feasibility of thermoelectric energy generation from a diver's breath. The prototype functioned under thermoelectric principles which produced electrical power where there is a temperature difference. In this case the temperature difference exists between the cold sea water and the relatively warm diver's breath.

10.2.1 Brief Design Specification

- The prototype must produce 50 microwatts of power or more.
- The prototype must harvest power from the diver's breath.
- The prototype must not be overly large as to obstruct diving.
- The prototype must be waterproof however it will be pressure balanced so does not need to withstand deep sea pressures.
- The prototype must provide a continuous reliable power supply.
- The prototype must not obstruct breathing, or make breathing more difficult and the work of breathing must still comply with CE EN14143:2003.
- Heat loss to the "scrubber" must be minimised.

10.3 The design

The design for the prototype focused around creating a waterproof casing for the thermoelectric generator that allowed; optimal exposure to both thermal environments, air flow through the casing and a removable but waterproof lid. An exploded view of the designed parts can be seen in figure 9.

10.3.1 Details

At the core of the design are the two heat sinks and the thermoelectric generator. The casing uses two lofted extrusions (extensions to the sides of the casing to promote smooth air flow) to connect up to the rebreather tubing at air inlet and outlet Figure 11. These allow smooth air flow over the heat sinks. The upper heat sink and the TEG sit inside designed steps inside the casing. The lower heat sink is glued onto the underneath of the casing in the hole shown in figure 12 via a two part resin glue. Thermal paste is placed on both sides of the TEG to improve thermal contact. The TEG and upper heat sink are then clamped down onto the lower heat sink by the clamp bars shown in figure 13. The clamping improves the transfer of heat with higher heat transfer with higher pressure clamping (Custom Thermoelectric, n.d.). The maximum clamping pressure rating on this particular TEG was 1 (Mpa).

The Lid was bought separately and the casing was designed to fit the waterproof seal on the Lid Figure 12 shows the slots which the lid clamps down onto.

Wires ran out through the wire hole shown in figure 10 which was potted once a dual cored wire had been connected up to the TEG.

10.4 Materials and manufacture

The casing was manufactured using the Object Eden 250 3D printer in Plymouth University. This machine prints to a high tolerance needed for the waterproof parts.

The clamp bars were manufactured by the maker bot 3D printers as they did not require the same quality as the casing and this was the cheaper option.

Parts				
Items	Two Heat sinks	Thermoelectric generator	Thermal Paste	Screws Nuts and potting material
Part No	104-092	765-0056	217-3835	Supplied by Plymouth university
Details	originally intended for Flood LED lighting however they were of the right size and shape to be used for this project	The TEG was bought after creating a graph comparing the larger ones cost to their power generating potential shown in figure 8	<p>FIGURE 8 TEG SELECTIONG GRAPH</p>	

10.5 Manufacturing Limitations

The Object Eden printer had 2 issues. Firstly the material ran out during printing of the first casing resulting in only half a case being built shown in figure 9.

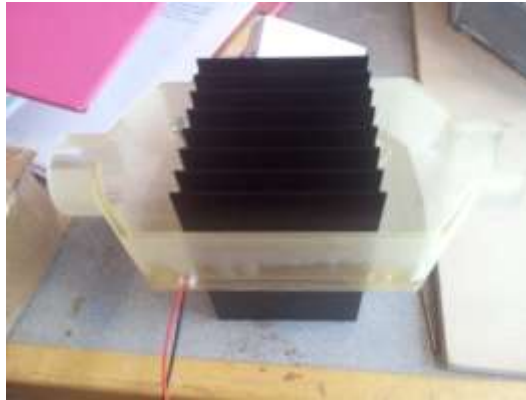


FIGURE 9 DEFECTIVE PART

Secondly the Printer produced defects in lip of the casing possibly to do with the small thickness of the “lid clamp slots” shown in figure 12. The design was amended however it was too expensive to produce another defect free case as the printing material is very expensive. Therefore vacuum bag gum sealant tape was used to seal the Lid on and ensure the defects did not cause the casing to leak.

For future prototyping I would recommend using a machined block of material for the casing as this would be much cheaper and less likely to incur defects however would require more time at the design stage to produce workable manufacturing drawings.

10.6 Design Drawings

Renders from the CAD can be seen below along with details describing the design of key components.

Exploded View

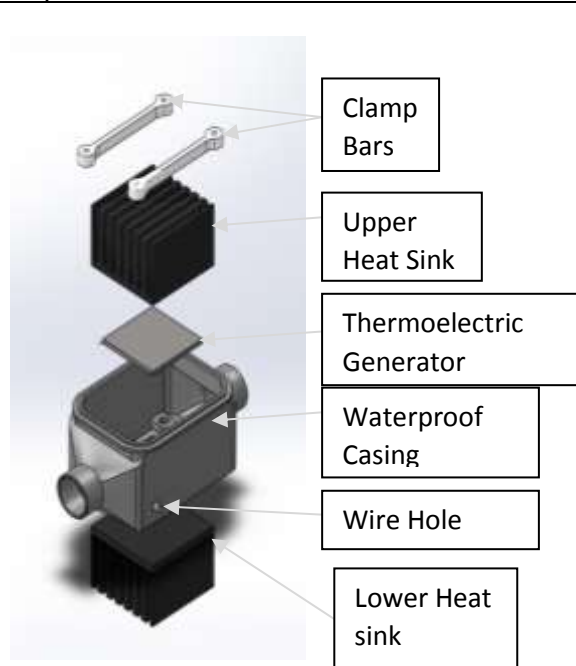


FIGURE 20 EXPLODED VIEW OF PROTOTYPE

Casing Top View

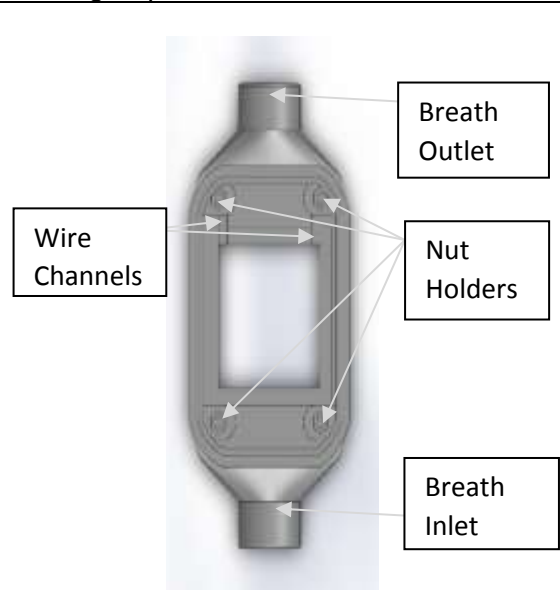


FIGURE 31 TOP VIEW OF PROTOTYPE

Casing Bottom View

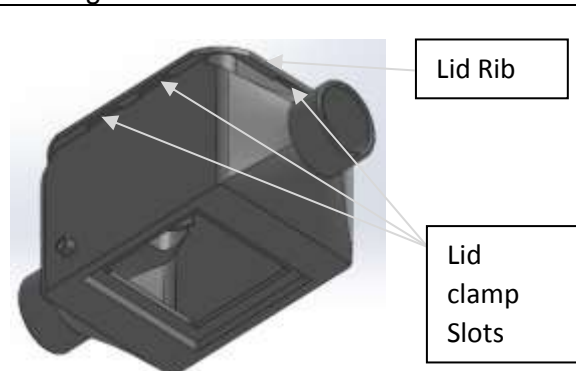


FIGURE 42 UNDERSIDE OF PROTOTYPE

Clamp Bars

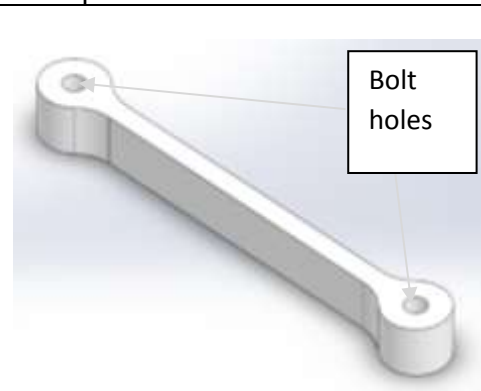


FIGURE 53 CLAMP BARS

Scale

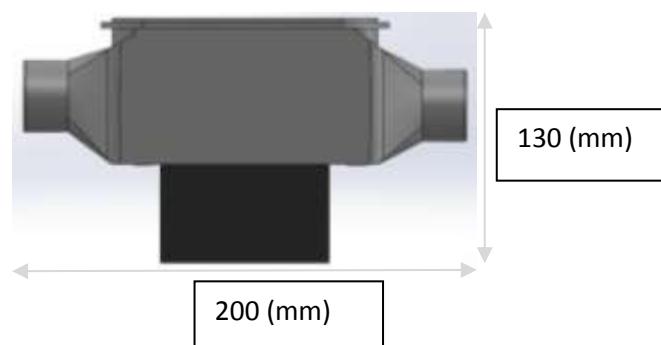


FIGURE 64 SCALE OF PROTOTYPE

10.7 Design Future recommendations

For the fully functioning prototype there will be no need for a removable lid therefore the design can be in a fully sealed case which will simplify the design improving its reliability and insulation properties.

To improve the heat transfer from the breath to the water a cylindrical Heat sink and TEG arrangement would be optimal however may be expensive in manufacture due to specialised parts. A compromise would be to use 4 TEG in series with 8 heat sinks on each side of the casing this could result in more heat being removed from the diver's breath.

Another recommendation would be to create a canister for the soda lime out of thermoelectric generators as this is where the temperature is at a maximum in the rebreather system however extensive research would have to be conducted on the effects of the cooling on the soda lime reaction caused by the TEG and its effect on duration of diving.

11 Experiment

11.1 Introduction

An experiment was carried out on the prototype device described above to determine its feasibility as an energy harvesting device. The device was placed in cold water and hot breath was breathed through the Rebreather. Steady state power output was 35 (mV) over a resistance of 0.6 (ohms) resulting in a power output of 3 (mW).

11.2 Aims

Measure power harvested by a thermoelectric generator powered by breath. And investigate the relationship between the power generated and the temperature of the air in the rebreather loop.

11.3 Methodology

Here the Equipment and method used for carrying out the experiment shall be described the experimental set up can be seen in figures 19, 20 and 21.

11.3.1 Apparatus

A list of the equipment used can be seen below

- Explorer Rebreather
- Soda Lime
- Energy harvesting prototype described above
- Thermocouple Data Logger
- Thermocouple Wire
- NI myDAQ measurement and instrumentation device
- Electrical Cabling and connectors
- 6 ohm Resistor
- Computer
- Bucket

- Ice
- Duct/electrical tape
- Wire strippers

11.3.2 Set up

Experimental Layout

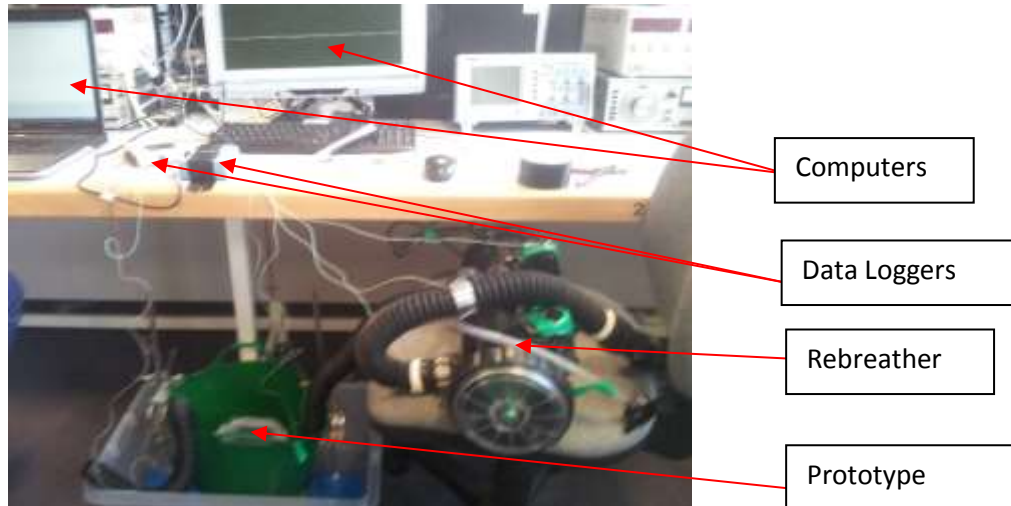


FIGURE 75 EXPERIMENTAL SET UP

Prototype

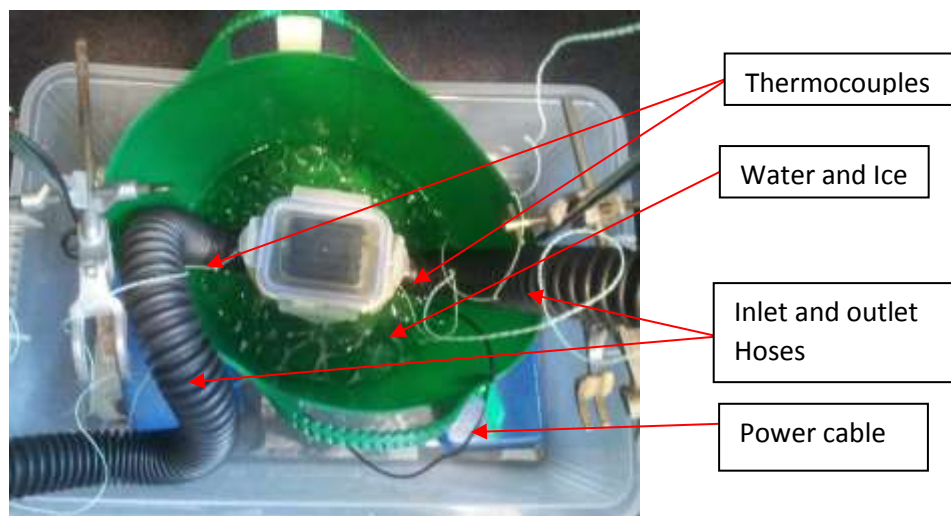


FIGURE 16 EXPERIMENTAL PROTOTYPE

Rebreather

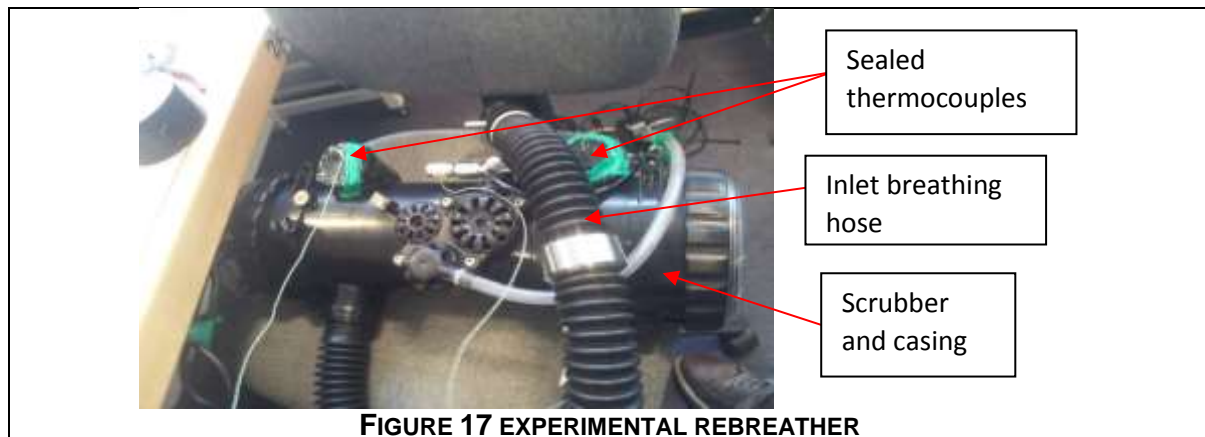


FIGURE 17 EXPERIMENTAL REBREATHER

11.3.3 Execution

1. Attach thermocouples to; breath inlet at mouthpiece, Scrubber inlet, Scrubber outlet, prototype Inlet, prototype outlet, ambient air and in the water.
2. Fill scrubber canister with soda lime ensure canister is properly filled.
3. Press Scrubber into the Rebreather loop.
4. Connect up the My DAQ data logger over the resistor.
5. Block off all air exits and blow through breathing tube to check for leaks and correct as necessary.
6. Tape down any electrical equipment to prevent anything falling into the water.
7. Fill bucket with water and Ice to a level that covers the bottom heat sink.
8. Place the prototype into the water with the bottom heat sink facing downwards and fix in place.
9. Start both data logging software's simultaneously taking measurements every 1 second for the power and 2 seconds for the thermocouples.
10. Constantly breathe through Rebreather loop for 2.5 hours.
11. Stop breathing and continue to measure data until it reaches a 0 value for the power output.

11.3.4 Safety

1. Special training is required to operate a closed circuit Rebreather safely. As the subject did not have such training the apparatus was run open loop, i.e., fresh air was drawn in on each breath, so regulation of the oxygen content was not necessary. Exhaled air was then passed through the experimental apparatus.
2. Ensure electrics do not come into contact with water by taping down electrics.

11.4 Variables

Dependent

- Voltage out from the thermoelectric generator.
- Temperature at each of the thermocouple measure points throughout the Rebreather and prototype.

Independent

- Breathing and not breathing through the Rebreather loop.

Fixed

- The resistance of the load.
- Resistance in the wires.
- Water temperature.
- Ambient air temperature.
- The ambient air pressure.
- The depth the prototype was underwater.
- The rate of breathing.
- Quantity of soda lime.

11.5 Prediction

There should initially be no power generated at the start of the breathing as the heat sink will take time to warm. Then a small amount of power should be generated based solely on the diver's breath temperature minus losses throughout the piping. After roughly 20 minutes the soda lime should have heated up (due to the exothermic reaction that takes place when it removes carbon dioxide from the air. Full equation is $\text{CO}_2 + \text{Ca}(\text{OH})_2 \rightarrow \text{CaCO}_3 + \text{H}_2\text{O} + \text{heat}$ (in the presence of water) (Wikipedia, 2015) (Chemical Book, 2010)) and caused significant increase in the air temperature at inlet to the prototype. The result of this should be a steady increase in voltage measured as the soda lime compound produces more heat. This increase in temperature for the soda lime should reach a steady state after an extended period of time roughly an hour resulting in a constant temperature at entrance to the prototype and therefore a constant voltage. Once the breathing is stopped the power should steadily return back down to a zero value over a small time period.

The mathematical models predicted that over a 10 degree temperature differential expected in the experiment there would be around 0.03 W of power being generated at around 0.5 (V).

11.6 Results

Results shall be displayed graphically due to the large amount of data points collected and to more easily see trends.

Current is calculated as a function of voltage and resistance. Power is calculated as a function of voltage and amplitude.

11.7 Graphs

The graphs produced from the experiment can be seen below.

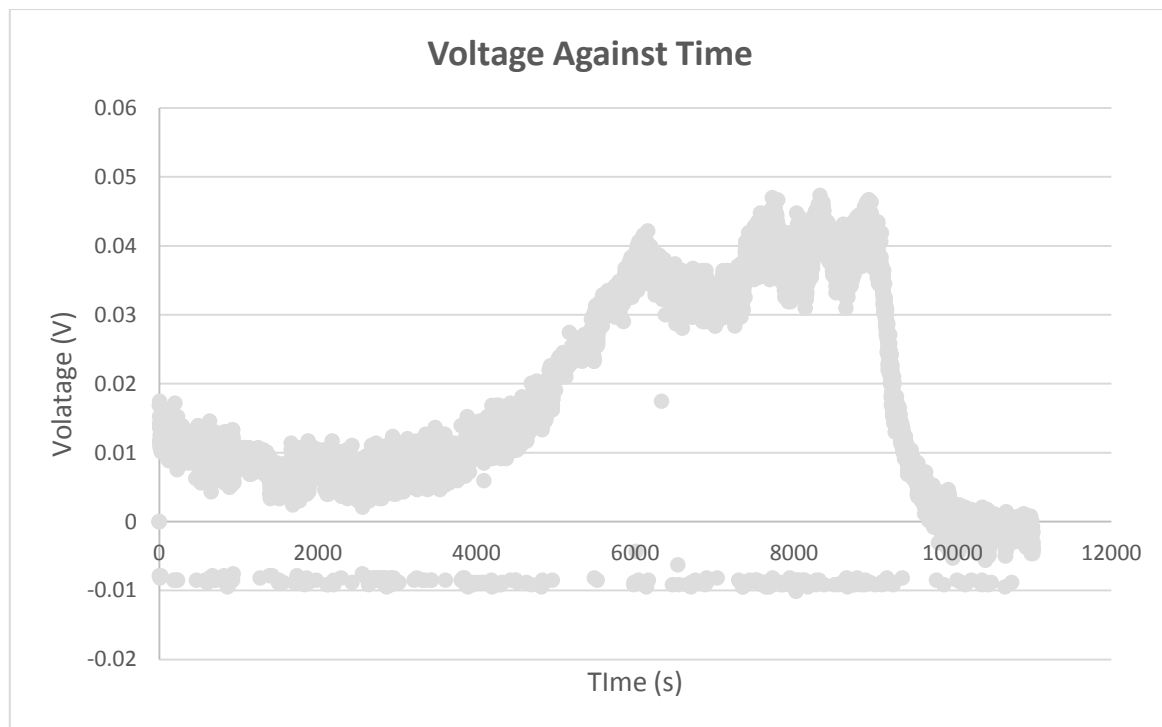


FIGURE 18 EXPERIMENT VOLTAGE GRAPH

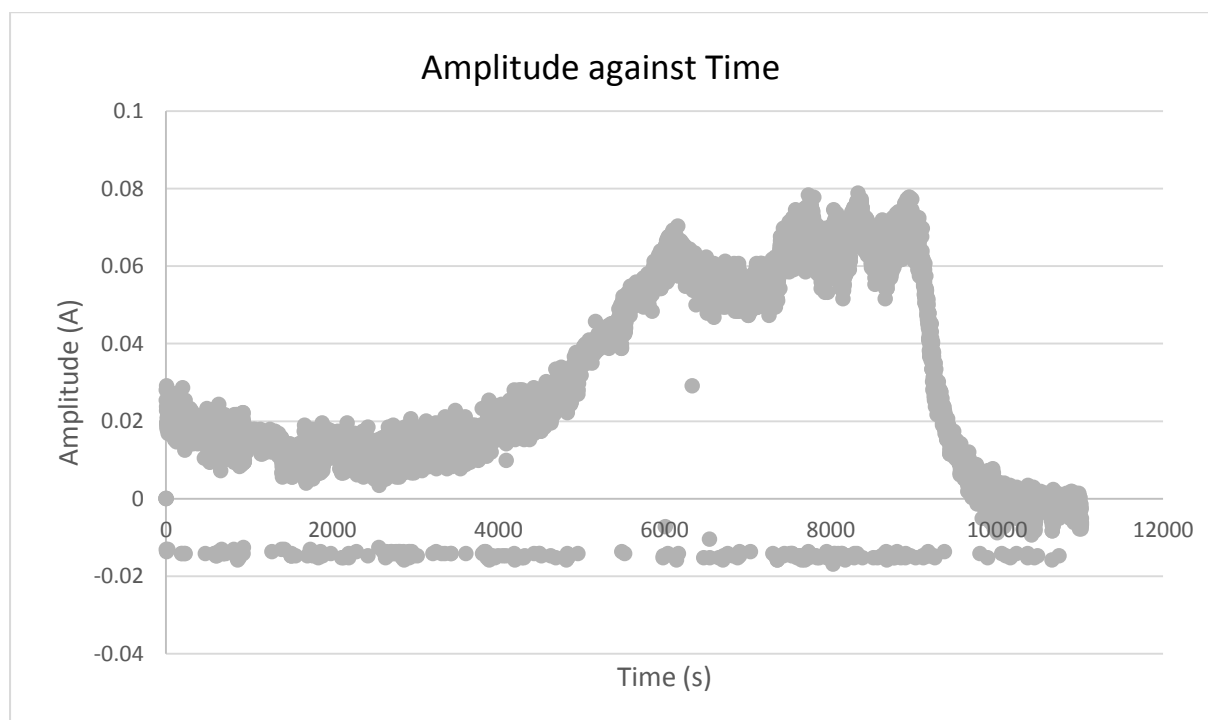


FIGURE 19 EXPERIMENT AMPLITUDE GRAPH

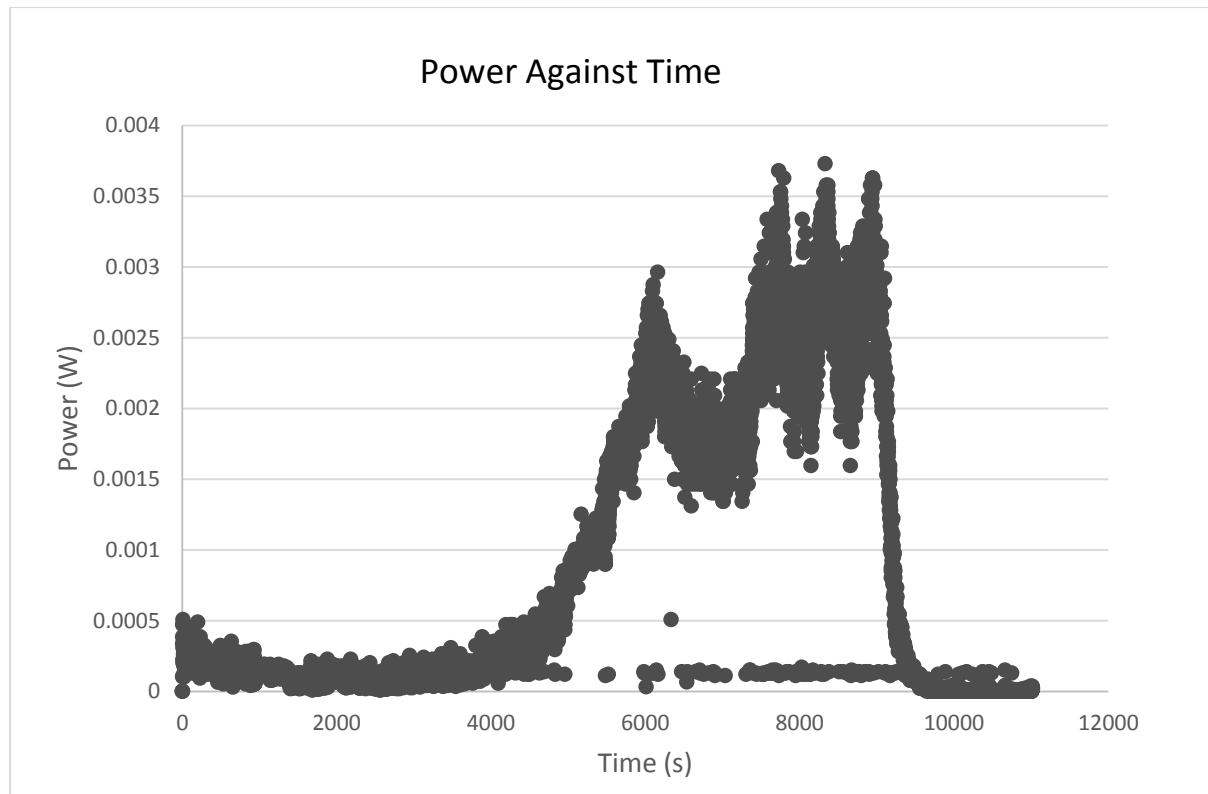


FIGURE 80 EXPERIMENT POWER GRAPH

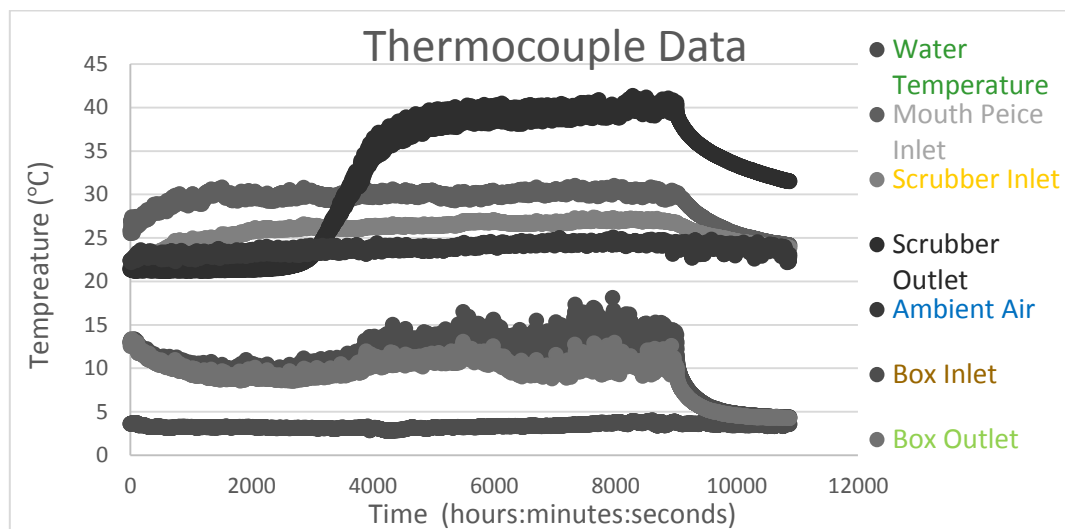


FIGURE 91 EXPERIMENT THERMOCUPLE GRAPH

11.8 Conclusion

11.8.1 Description of the results

The voltage against time graph shown in figure 18 demonstrates a decreasing shallow slope in voltage from an average value of 0.02(V) at 0 seconds to an average value of 0.01(V) at 2000 seconds. The data then remains constant till 4000 seconds. The slope then changes to a positive but still shallow gradient back up to a value of 0.02(V) at 5000 seconds. The graph then exhibits a steeper positive

gradient continuing to a voltage value of 0.04 (V) at 6000 seconds. The graph then oscillates around 0.05(V) and 0.03 (V) till 9500 seconds. The graph then experiences a sharp negative gradient to a value of 0(V) at 10000 seconds and then remains at 0 (V) till the end of the experiment.

The graphs shown in figure 18, 23 and 24 exhibit similar behaviour as they are function of the voltage.

The thermocouple data graph shown in figure 21 demonstrates the temperatures throughout the Rebreather. The data lines that are of interest are the Scrubber outlet and the box inlet and outlet. The other Data lines remained mostly constant with a slight positive gradient throughout the experiment. Note that the water temperature remained at a constant 3.5 Degrees C throughout.

The Scrubber outlet Data line demonstrates a constant temperature of 21-21.5 degrees C from 0 seconds to 3000 seconds. The data then exhibits a steep positive linear gradient to a value of 37 degrees C at a time of 3800 seconds. The data then shows a very shallow positive gradient to a value of 40 degrees at 9500 seconds. The data then shows a sharp negative slope to a value of 33 degree c at the end of the experiment.

The box inlet data line shows a shallow negative correlation from 13 degrees c to 10 degrees c from 0 to 1500 seconds. The data then shows a shallow positive correlation from 10 to 15 degrees C from 1500 to 9500 seconds. The data then takes a sharp negative correlation to 5 degrees c at 10000 seconds and remains at this value till the end of the experiment.

The box outlet data exhibits similar behaviour however at 4000 seconds it fluctuates around 10 degrees C until 9500 seconds.

The amount of power generated is roughly 0.2 (mW) at 10 (mV) and 16 (mA) without aid from the Scrubber and 2.5 (mW) at 35 (mV) and 58 (mA) and when the reaction reaches steady state.

11.8.2 Scientific explanation for the results

The negative correlation shown in the power graphs at the start is due to large initial temperature difference between the water and the uncooled heat sinks when the prototype is placed into the bucket. This initial temperature difference is larger than the temperature difference caused by breath over the heat sink initially and therefore produces a negative gradient.

The voltage then becomes steady state as the breath heats the upper heat sink and the water cools the lower heat sink unaided by the exothermic reaction from the scrubber. This is shown on figure 21 as the scrubber outlet temperature does not exceed ambient till 4000 seconds.

The steep positive correlation is caused by the exothermic reaction from the scrubber heating the breath as it goes through the canister. The positive correlation from the thermocouple graph is roughly 2200 seconds ahead of the voltage graph this could be due to the temperature increase taking time to transfer into the air and also transfer through the heat sink to the thermoelectric generator.

The voltage then reaches steady state as the exothermic reaction reaches its peak temperature this may be due to it removing a maximum amount of CO₂ from the breath and therefore not being able to react further. The thermocouple graph is showing a small positive gradient however this is likely due to the heat warming the casing rather than producing more heat from the reaction.

The sharp negative gradient is due to the breathing through the Rebreather loop being stopped.

The box inlet and outlet temperatures are much lower than the scrubber outlet temperature. This could be due to the fact that they were underwater at the time so heat could be lost to the pipes leading to the prototype. The thermocouples may have come into contact with the box casing and therefore would have been measuring the surface temperature rather than the air temperature which would explain why they increased much more slowly.

There are many data points at -0.01 these extraneous data points are the result of movements during the experiments which could cause connections to move or faults to occur within the MyDAQ data logger.

11.8.3 Conclusion from results

From this experiment it can be seen that the breath is having a significant impact on the power generated from the thermoelectric generator. Further the effect of the exothermic reaction has a large effect on the power generated (more than 3 times the power generation).

Reliable power was always generated whilst there was breath moving through the loop however there are negative spikes caused by movement which could affect the reliability of the device as it would need to be in a moving environment in practice. These could perhaps be eliminated with more secure electrical connections.

11.8.4 Do results agree with the prediction?

Results follow the same pattern as predicted however it took longer for the exothermic reaction to take place than originally anticipated; this may be due to the Rebreather being used as an open loop during the experiment. The soda lime also reacts more when under pressure and this experiment was done at ambient conditions.

The numbers themselves were much lower than predicted from the mathematical models; this could be due to a smaller temperature difference being maintained over the TEG than originally expected due to losses of heat through the piping (Box inlet temperatures are much lower than scrubber outlet temperatures around a 30 degree C difference) and the low thermal conductivity of air (shown in the small temperature difference between box inlet and outlet around 2 degrees C).

Evaluation

11.8.5 Validity

The experiment was a valid way of determining the feasibility of energy harvesting from breath and was a valid way of determining if the exothermic reaction had an

effect on the power generated. However the Rebreather and piping was not submerged under water and the breathing loop was open instead of closed therefore the validity of the actual numbers may not represent a diver underwater and further tests can be carried out to take the project further. The water temperature was very low in the test 3.5 degrees C in reality the water could have a vast range of temperatures from 0 – 25 degrees C which may result in lower power being produced therefore future test could include a range of water temperatures.

The high pressure experienced underwater could have a large effect on the air density and temperature of the diver's breath this would undoubtedly change the amount of power generated by the TEG. The experiment was only run at atmospheric conditions therefore may not be valid for a diver under pressure.

A brief description of previous similar experiments can be found in appendix D.

11.8.6 Accuracy and precision

Using data logging was essential in the methodology of this experiment as a large amount of results needed to be taken over a long duration. Further data logging is a highly accurate way of measuring figures (as can be seen in the precision error below) which was necessary for measuring such small voltages.

The myDAQ had $\pm 0.0001(V)$ error.

The Thermocouple Data logger had ± 0.01 *degrees C* error.

The disadvantage of Electronic data logging is the large initial time taken to setup the experiment and then the reliability of the equipment. The software crashed a number of times due to the large amount of data it needed to collect which added onto the time taken to perform the experiment.

The thermocouple Data logger was 2 degrees below a handheld thermocouple measuring device when measuring ambient air temperatures therefore it is possible there is a 2 degree systematic error in all thermocouple measurements.

11.8.7 Future recommendations

In order to take this project further I would recommend using the Ansti testing facilities to run an underwater test over a 5 hour period at different pressures and different water temperatures and breathing rates. Also placing the prototype at different points in the Rebreather loop may result in more effective energy harvesting. Using thermally insulating sleeves over the piping would decrease wasted heat loss through the pipes. If this prototype were to be used in the divers Kit a voltage booster would need to be incorporated into the circuit as the voltage is too low to be useful in its current state. The LTC3108 Energy harvesting breakout board would be ideal for this situation due to its unique functioning at low voltages found at (<http://harizanov.com>).

12 Project conclusion

The minimum target for power was 50 microwatts to power the low power equipment on the diving system. The prototype generated 0.2 (mW) without aid from the scrubber and 2.5 (mW) and when the reaction reaches steady state. Both these

values are higher than the minimum power value specified by Avon therefore thermoelectric energy harvesting within a divers Rebreather system is feasible.

The mathematical models and previous documented experiments predicted higher values than the experiment produced which suggests that refinements in the prototype to capture more of the thermal energy and transfer it over the TEG would result in even more power being produced.

13 References

AAvid Thermalloy, n.d. *docs-europe.electrocomponents*. [Online]
Available at: <http://docs-europe.electrocomponents.com/webdocs/0978/0900766b80978dea.pdf>
[Accessed 09 04 2015].

AAvid Thermalloy, n.d. *How a Heat pipe works*. [Online]
Available at: <http://www.aavid.com/product-group/heatpipe/operate>
[Accessed 02 12 2014].

Beadsell , L., 2009. *MCEM Part A*, s.l.: Royal society of Medicine Press.

Carpenter, D. A. & Buttram, M. J., 1998. *Breath Temperature an Alabama Perspective*. Alabama: International association for chemical testing.

Cengel, Y. A. & Boles, A. M., 1998. Thermodynamics an engineering approach. In: America: McGraw-Hill, pp. 644-647.

Chemical Book, 2010. *Soda Lime*. [Online]
Available at:
http://www.chemicalbook.com/ChemicalProductProperty_EN_CB7289231.htm
[Accessed 26 04 2015].

Chung, D. Y. et al., n.d. *Complex bismuth chalcogenides as thermoelectrics*. s.l., s.n., p. 459.

Custom Thermoelectric, n.d. *Application Notes*. [Online]
Available at: <http://www.customthermoelectric.com/>

Datt, P., 2014. Latent Heat of Condensation. *Encyclopedia of earth sciences*, pp. 702 -703.

Delnavaz, A., 2012. *Electromagnetic micro-power generation for energy harvesting from breathing*. Montreal , IECON 2012 - 38th Annual Conference on IEEE Industrial Electronics Society.

Dewan, A., Ay, S. U., Karim, M. N. & Beyenal, H., 2014. Alternative power sources for remote sensors: A review. *Journal of Power Sources*, Volume 245, pp. 129-143.

Dewan, A., Nazmul , K. & Beyenal, H., 2013. Alternative power sources for remote sensors. *Journal of power sources* , pp. 129-143.

E How, n.d. *How to calculate velocity of air in a pipe*. [Online]
Available at: http://www.ehow.com/how_8477084_calculate-velocity-air-pipe.html
[Accessed 02 12 2014].

Engineering toolbox, n.d. *Pipe Fluid Flow Velocity*. [Online]
Available at: http://www.engineeringtoolbox.com/pipe-velocity-d_1096.html
[Accessed 2 12 2014].

European Thermodynamics Limited , n.d. *Radio Spares*. [Online]
Available at: <http://docs-europe.electrocomponents.com/webdocs/1110/0900766b81110d9c.pdf>
[Accessed 09 04 2015].

Ferrotec, 2001. *Thermoelectric Technical Reference- Power generation*. [Online]
Available at: <https://thermal.ferrotec.com/technology/thermoelectric/thermalRef13>
[Accessed 10 04 2015].

Ferrotec, n.d. *Basic principles of thermoelectric materials*. [Online]
Available at: <https://www.ferrotec.co.uk/technology/thermoelectric/thermalRef02/>
[Accessed 2014 11 30].

Goldsmid, J. H., 2014. Bismuth Telluride and Its Alloys as Materials for Thermoelectric Generation. *mdpi materials*.

Haywood, R. W., 2005. *Thermodynamic tables in SI units*. 3rd ed. Cambridge: Press Syndicate of the University of Cambridge.

Hopkins Medicine, n.d. *Hopkins Medicine*. [Online]
Available at:
http://www.hopkinsmedicine.org/healthlibrary/conditions/cardiovascular_diseases/vital_signs_body_temperature_pulse_rate_respiration_rate_blood_pressure_85,P00866/
[Accessed 02 12 2014].

Kryotherm, n.d. *Thermoelectric products and thermoelectric power generation solutions*, s.l.: Kryotherm.

Leonov, R. J. M. V., n.d. *Thermoelectric Generators on Living Beings*, s.l.: Interuniversity Microelectronics Center.

Miljkovic, 2014. *Email*. s.l.:s.n.

Miljkovic, N., Preston, D. J., Enright, R. & Wang, E., 2014. Jumping-Droplet electrostatic energy harvesting. *Applied Physics Letters*.

Miljkovic, N., Preston, Enright & Wang, R., 2013. Electrostatic charging of jumping droplets. *Nature Communications*, Volume 4, p. 1.

O'Halloran, D. S., 2014. *Power and Efficiency Measurement in a Thermoelectric Generator*. s.l., American Society for Engineering Education,.

Paradiso, J. A. & Starner, T., 2005. Energy scavenging for mobile and wireless electronics. *IEEE Pervasive Comput.*, 4(1), pp. 18-27.

Radio Spares, 2013. *docs-europe.electrocomponents..* [Online]
Available at: <http://docs-europe.electrocomponents.com/webdocs/02b8/0900766b802b8c29.pdf>
[Accessed 09 04 2015].

Rowe, M., 1994. Thermoelectric Generators as Alternative sources of low power. *Renewable energy*, Volume 5, pp. 1470-1478.

Sentinel rebreather Manual, n.d. *Avon Protection Underwater systems*. s.l.:Avon Industries.

Tellurex, 2010. *Tellurex*. [Online]
Available at: <https://tellurex.com/>
[Accessed 14 04 2015].

U. S. Department of the Navy, Naval Sea Systems Command, 1974. *U.S. Navy Diving Manual: Mixed-gas diving*. s.l.:Military Studies Press, 2012.

U. S. Department of the Navy, Naval Sea Systems Command, 2008. *U.S. Navy Diving Manual*. s.l.:Military Studies Press, 2012.

Wikipedia, 2014. *Breathing*. [Online]
Available at: <http://en.wikipedia.org/w/index.php?title=Breathing&action=history>
[Accessed 02 12 2014].

Wikipedia, 2014. *Heat pipe*. [Online]
Available at: http://en.wikipedia.org/w/index.php?title=Heat_pipe&action=history
[Accessed 02 12 2014].

Wikipedia, 2015. *Rebreather*. [Online]
Available at: <http://en.wikipedia.org/wiki/Rebreather>
[Accessed 26 04 2015].

Wikipedia, 2015. *Soda Lime*. [Online]
Available at: http://en.wikipedia.org/wiki/Soda_lime
[Accessed 26 04 2015].